



Modeling and optimization of the removal of chlorpyrifos and organics reduction from wastewater by Ag/AgBr/TiO₂ using the central composite design (CCD)

Poh Lin Lau*, Augustine Chioma Affam

Department of Civil Engineering, University College Of Technology Sarawak, No 1., Jalan Universiti, 96000 Sibul, Sarawak, Malaysia, emails: plinlau20@yahoo.com (P.L. Lau), augustine@ucts.edu.my (A.C. Affam)

Received 23 April 2019; Accepted 11 September 2019

ABSTRACT

Chlorpyrifos (CPF) is an organophosphate that has strong recalcitrant properties and may not fully degrade in the conventional industrial wastewater treatment plant. The visible light photocatalyst is one of the emerging methods proposed to enhance the biodegradability of pesticide wastewater. This study investigated the application of visible-light photocatalyst (Ag/AgBr/TiO₂) for the degradation of CPF pesticide wastewater. Experiments were designed and optimized using the central composite design of the response surface methodology. The effects of three independent parameters including dosage of Ag/AgBr/TiO₂, pH and reaction time were studied. The maximum chemical oxygen demand (COD) removal predicted was 78.3% and the actual or experimental COD reduction was up to 75.8%. The predicted and actual COD removal was in close range and acceptable. The optimum operating condition of pH = 10, Ag/AgBr/TiO₂ dosage = 10 g L⁻¹ and reaction time of 70 min was obtained. This study showed that prepared visible light catalyst was efficient in the degradation of CPF contaminated wastewater.

Keywords: Visible light photocatalysis; Chlorpyrifos wastewater; Central composite design (CCD); Optimization; Modeling; Chemical oxygen demand (COD)

1. Introduction

Chlorpyrifos (CPF) was first introduced to the market in 1965 and it became the most widely used pesticide in the world. It was registered for use in more than 900 various pesticide formulations including the emulsified concentrate, granule, wet powder, and dispersible granule [1,2]. It is widely used to control different insects in agriculture [2]. It is toxic to non-target organisms, including humans and may damage the lungs and central nervous system, causing autoimmune disorders, and also retard mental development [2]. In addition, CPF has been detected in rivers [3] due to improper handling of organophosphate insecticide by large-scale pesticide manufacturing industries and has resulted

in the deaths of mammals [4]. Low-to-medium concentration CPF pesticide in water (<500 mg L⁻¹) may cause adverse effects on human health [5]. Due to its recalcitrant properties, it is difficult to decompose naturally in water.

Over the past few decades, various wastewater remediation has been introduced to degrade water pollutants, including biological treatment [6], coagulation/flocculation [7] and advance oxidation processes (AOPs). AOPs are recognized as an environmentally friendly technology where powerful oxidants such as hydroxyl radicals (OH) are produced and enable the conversion of the water pollutants into less harmful end products such as carbon dioxide, water and inorganic species [8]. Photocatalyst can be activated by free

* Corresponding author.

and abundant solar irradiation and has been widely studied in recent years as it can oxidize the pollutants effectively at low energy cost [9,10].

Semiconductor photocatalyst is getting increased attention due to their great potential in solving environmental and energy issues ranging from decomposing organic pollutants, water splitting and artificial photosynthesis by harvesting the solar light energy [11]. Titanium dioxide was chosen as the primary photocatalyst because the anatase form of TiO_2 is most active to the photon, non-toxic and highly active [12]. Due to the wide bandgap of TiO_2 (3.2 eV), it only absorbs light in the ultraviolet (UV) region with a wavelength of less than 400 nm [13–15] and that is only 5% of the solar spectrum [16] and thus limits its photocatalytic efficiency. Thus, lots of efforts are being done to enhance the photoreactivity of TiO_2 .

Nobel metals such as silver, gold, and platinum are used as dopant to modify the surface of TiO_2 due to their surface plasmon resonance (SPR) [17,18] as they can improve the absorption of light in the visible light region and form the Schottky barrier on the surface of TiO_2 to suppress the recombination of electron-hole pairs as noble metals acts as an electron trapper [19,20]. Silver/silver halide composite photocatalysts have been recognized as promising and stable photocatalytic under visible light [19,21]. For example, Ag/AgBr/ TiO_2 has been applied to degrade dye such as methylene blue [22]. The study reported that the photodegradation properties of Ag/AgBr/ TiO_2 were better than bare TiO_2 nanopowder and Ag/AgBr powder. Besides, the recycling runs experiment showed the photocatalytic stability of Ag/AgBr/ TiO_2 . The method used in the preparation of Ag/AgBr/ TiO_2 was the Sol–Gel method and was thereafter applied in the photodegradation of methyl orange. It was found that the performance of modified TiO_2 was better than mesoporous TiO_2 and commercial TiO_2 [23]. Another photo degradative properties of Ag/AgBr/ TiO_2 was tested on methyl orange where 162.4% Ag/AgBr/ TiO_2 exhibited the highest dye removal [24]. Other than dyes, Ag/AgBr/ TiO_2 has been applied in the decomposition of *Escherichia coli* in water and it was reported that reactive radicals such as $\cdot\text{OH}$, O_2^- , holes and Br^0 caused the bacteria to die [25].

The design of experiment is used to study the relationships between factors affecting a process and obtain the results of the experiment. One factor at a time is the traditional experimental and analytical method. This is done by changing one parameter while others are kept constant. It is very time consuming, incurs high costs as it requires a large number of experiments and it does not study the interactive effects among the selected parameters [26]. Response surface methodology (RSM) was developed as a combination of mathematical and statistical methods to design experiments, develop models with the interactions of parameters and optimize the process [27–29]. RSM has been successfully employed to optimize the removal of various pesticides in wastewater such as methyl parathion [7], profenofos [30], abamectin [31], acetamiprid [32], and malathion [33].

There is no reported work on the RSM optimization of CPF for chemical oxygen demand (COD) removal by visible light-activated Ag/AgBr/ TiO_2 . This study focused on photodegradation of CPF using Ag/AgBr/ TiO_2 and the effects of different parameters: such as catalyst load, initial pH and

reaction time on the reduction of COD and CPF concentration was optimized by using the central composite design (CCD).

2. Experimental setup

2.1. Materials

Silver nitrate (AgNO_3) was purchased from Bendosen, potassium bromide (KBr) was purchased from BDH (England) and titanium(IV) oxide was purchased from Merck Company (Germany). CPF with concentration 38.7% w/w was purchased from a local agriculture store (Bintangor, Sarawak).

2.2. Preparation of Ag/AgBr/ TiO_2

Impregnation–precipitation–photoreduction [9] was selected to prepare the composite Ag/AgBr/ TiO_2 . 1 g of TiO_2 powder was impregnated in 20 mL of 0.0053 mol AgNO_3 for 30 min. Thereafter, 20 mL of 0.006 mol KBr with a concentration greater than AgNO_3 was added drop by drop to the mixture and stirred continuously for the range 60 min to induce the precipitation of deposited AgNO_3 into AgBr. The reduction of AgBr was carried out via irradiation by visible light ($420 \text{ nm} < \lambda < 780 \text{ nm}$) for 90 min. Finally, the mixture was washed several times with distilled water and dried in a vacuum oven at 70°C [22]. The prepared samples were denoted by weight ratio Ag/AgBr/ TiO_2 . The catalyst was prepared at a 1:1 weight ratio of Ag: TiO_2 , which was calculated assuming that all of the AgBr was reduced to Ag, for simplicity.

2.3. Characterization of Ag/AgBr/ TiO_2

The surface morphology of Ag/AgBr/ TiO_2 was analyzed by scanning electron microscopy (SEM) (JEOL-6010PLUS/LV, Japan) and the atomic composition of Ag/AgBr/ TiO_2 was analyzed by energy-dispersive X-ray spectrometer (EDS) was carried out. X-ray diffractometer (XRD) with D8 Bruker, (Germany) operating at 40 kV and 40 mA using Cu $K\alpha$ radiation ($k = 1.5418 \text{ \AA}$) were used to characterize the crystal structure of photocatalyst.

2.4. Experiment

CPF pesticide wastewater was prepared using distilled water a fixed concentration of 200 mg L^{-1} [34] with some modification. The wastewater was selected by adding a mixture of 200 mg L^{-1} of CPF, starch (0.25 g L^{-1}), sodium acetate (0.25 g L^{-1}), ammonium chloride, NH_4Cl (0.08 g L^{-1}), potassium dihydrogen phosphate, KH_2PO_4 (0.12 g L^{-1}), dipotassium hydrogen phosphate, K_2HPO_4 (0.29 g L^{-1}), calcium chloride dihydrate, $\text{CaCl}_2 \cdot 2\text{H}_2\text{O}$ (0.035 g L^{-1}), magnesium sulphate heptahydrate, $\text{MgSO}_4 \cdot 7\text{H}_2\text{O}$ (0.045 g L^{-1}) and peptone (0.01 g L^{-1}). About 100 mL of the wastewater was put in a 250 mL beaker. The characteristic of CPF wastewater is shown in (Table 1). The pH of the solution was adjusted by adding either drops of 1 Molar sulphuric acid, H_2SO_4 or sodium hydroxide, NaOH. Thereafter, a certain amount of Ag/AgBr/ TiO_2 was added to the CPF wastewater and stirred for a certain time to ensure uniform mixing of the photocatalyst in the solution. The reaction mixture was carried out under room temperature of about $25^\circ\text{C} \pm 0.5^\circ\text{C}$ and in the visible light condition.

Table 1
Characteristics of CPF wastewater

Parameters	Amount
pH	7.2
Chemical oxygen demand (COD) (mg L ⁻¹)	1,270
Chlorpyrifos (mg L ⁻¹)	200

2.5. Analytical methods

At the desired time, 10 ml of CPF wastewater was taken out and centrifuged to immediately separate the treated CPF wastewater and Ag/AgBr/TiO₂. COD was used to analyze the reduction organics based on the Standard Methods [35] and the changes in the concentration of CPF fractions was analyzed by Agilent (USA) high-performance liquid chromatography (HPLC) using C18 column acetonitrile and HPLC water (70:30, v/v) was used as a mobile phase at a flow rate of 0.2 mL min⁻¹. The peak was observed at 220 nm.

2.6. Experimental design

Experiments were designed at low (-1), middle (0) and high levels (+1) of the process. Three parameters were the independent facts of the process. These were contact time, pH and photocatalyst dosage required to study the kinetic of the photodegradation of CPF wastewater as shown in Table 2.

3. Results and discussion

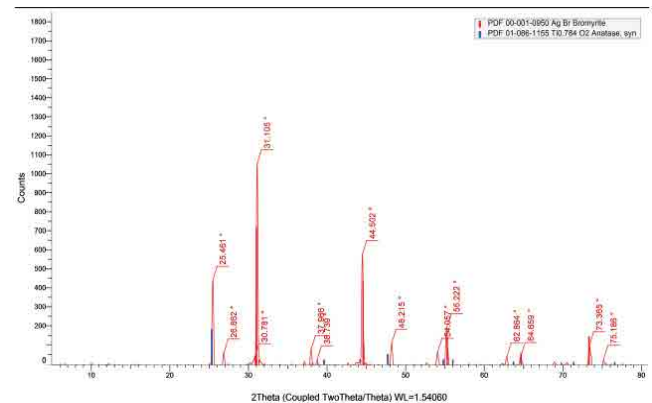
3.1. Characterization of Ag/AgBr/TiO₂

The X-ray diffraction (XRD) patterns of pure TiO₂ and Ag/AgBr/TiO₂ was obtained from 1 g of AgBr dopant sonicated with TiO₂ under 60 min precipitation time followed by 90 min irradiation time is shown in Fig. 1. In the XRD image, except the peaks of anatase in the TiO₂, the peaks at 26.7°, 31.1°, 44.5°, 55.1°, 64.6°, and 73.4° were formed at (200), (202), (222), and (420) reflection of AgBr [24,36,37]. Ideally, the peaks of Ag should be detected at 38.1°, 44.3°, 64.5°, and 77.4°. In this study, the only detected peaks were 44.5° and 64.6° which could be assigned as Ag and AgBr, respectively. The pure peak of Ag was difficult to see as it may have overlapped the anatase phase at 38.7° [38]. Other diffraction peaks of Ag could not be shown. This may be because of the low content of Ag, tiny particle size, poor crystalline structure and high dispersion [39]. The XRD illustrates clearly the presence of AgBr and TiO₂ but not Ag in the modified TiO₂ photocatalyst. Nevertheless, the existence of metallic Ag was further demonstrated by SEM-EDX analysis shown in Fig. 2.

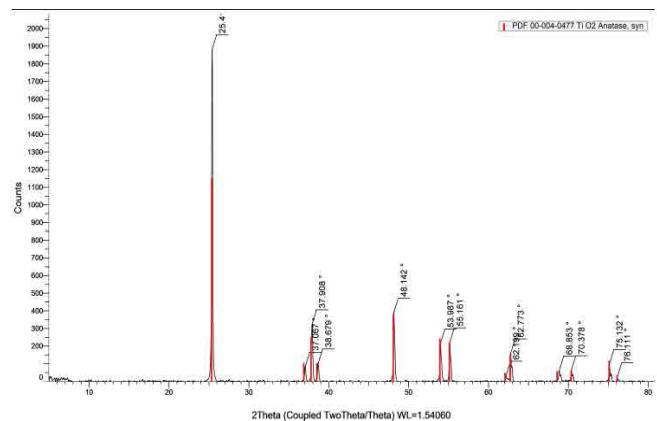
In Fig. 2, the irregular and dented surface of pure TiO₂ were irregular sizes during agglomeration. The agglomerates and the dents were diminished and replaced with regular powder formed surfaces. This may be due to the presence of Ag on the irregular surface of TiO₂ and decreased its specific surface area [24]. With the aid of EDS analysis, TiO₂ and O were the dominant elements that were found in TiO₂ with an estimated weight of 39.9% and 48.96%, respectively. The C element is attributed to the calibration carbon [13] and Zr peaks with a small amount were observed in the

Table 2
Central composite design (CCD)

Variables	Factor code	Levels		
		-1	0	1
pH	A	4.5	7.25	10
Contact time, min	B	70	125	180
Ag dosage, g	C	1	1.75	2.5



(a)



(b)

Fig. 1. XRD pattern for (a) pure TiO₂ and (b) Ag/AgBr/TiO₂.

EDS pattern, as the impurities found in the TiO₂ powder. EDX of Ag/AgBr/TiO₂ revealed that the samples consisted of Ag with a 14.46% weight. Since the weight percentage of Br was not showed, the mass ratio of Ag/AgBr/TiO₂ obtained was not comparable with the theoretically calculated value of Ag/AgBr:TiO₂ (1:1).

3.2. Model fitting and analysis

A total of 28 experiments were conducted based on the design expert (Table 3). Two replications were carried out for factorial points, one replication of axial point and six replications of the center point. Table 3 shows the independent

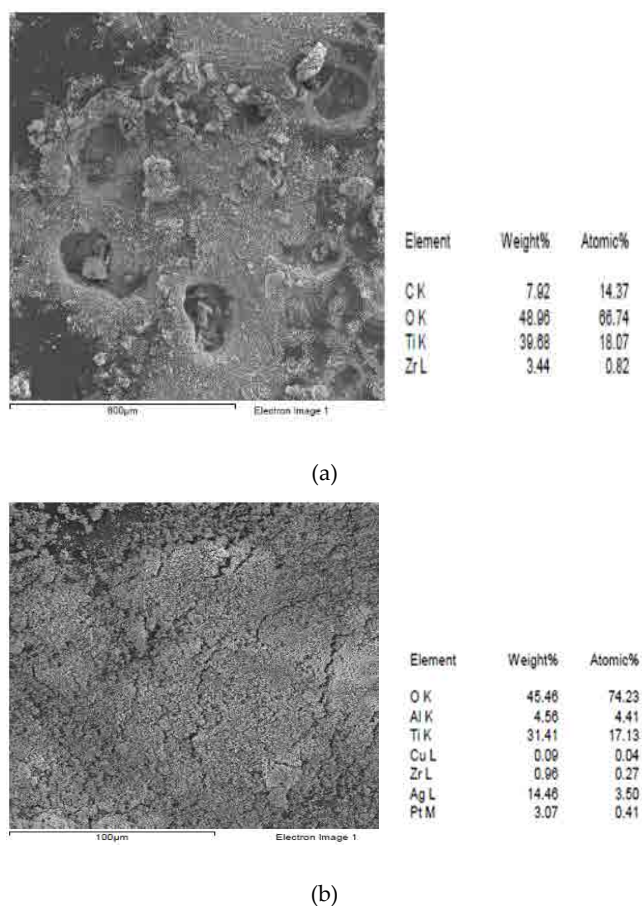


Fig. 2. SEM and EDX analysis for (a) pure TiO_2 and (b) Ag/AgBr/TiO_2 .

variables and experimental results of the CPF wastewater degradation by CCD. The design summary suggested that the 2FI model is the best-fitted model (Table 4). The model adequacy was further validated by analysis of variance (Table 5). The model F -value of 8.68 implied that the model was significant. There was only a 0.01% chance that an F -value this large could occur due to noise. The P -value of the model was less than 0.0001 indicates that the model was significant. The lack of fit value of 2.45 implied that the lack of fit is not significant relative to the pure error when P -value = 0.0732, which was more than 0.05. This indicated good predictability. Furthermore, the 2FI model had a low standard deviation of 1.54 and the predicted R^2 value 0.4469 is in reasonable agreement with the Adj R^2 value 0.6305. Based on (Table 6), the coefficient of the model for the response was estimated using multiple regression analysis techniques and the 2FI model was obtained. In terms of actual factors Eq. (1) expresses the COD removal with the effects of input factors, A , B , and C .

$$\text{COD removal (\%)} = 81.03 - 1.51A + 0.65B - 0.054C + 1.27AB + 0.34AC - 1.41BC \quad (1)$$

The significance of the parameter coefficients could be seen from Table 6. The coefficient is significant if the P -value

Table 3
Experiment design matrix and results for COD removal by CCD

Run	pH	Contact time (min)	Ag dosage (g)	COD removal (%)
1	4.5	70	2.5	84.5
2	7.25	125	1.75	80.2
3	7.25	125	1.75	80
4	10	70	1	77.9
5	7.25	125	1.75	79
6	10	180	2.5	80.2
7	12.75	125	1.75	79.1
8	7.25	125	1.75	80.6
9	10	70	2.5	80.5
10	1.75	125	1.75	83.2
11	10	70	1	76
12	10	180	1	82.7
13	4.5	180	1	83
14	10	180	1	80.5
15	7.25	235	1.75	85.2
16	4.5	180	1	78
17	4.5	70	1	83.1
18	10	70	2.5	78.6
19	7.25	15	1.75	78.6
20	7.25	125	3.25	80
21	4.5	180	1	85.5
22	7.25	125	1.75	80.4
23	4.5	70	1	82.7
24	4.5	180	2.5	81.7
25	4.5	70	2.5	86.9
26	7.25	125	1.75	79.5
27	7.25	125	0.25	80.2
28	10	180	1	80.9

is less than 0.05. “ A ” term (pH) was only significant model terms. Although the “ B ” term (contact time) has a P -value (0.0533) which was slightly greater than 0.05, it was kept as a relevant correlation because it had significant coefficients on COD removal when paired with other factors. The influence of the contact time and catalyst dosage had the highest significance with an F -value of 13.26 and a P -value of 0.0015.

3.3. Effects of the input factors on the photodegradation

This section describes the effect of the input factors such as pH and Ag/AgBr/TiO_2 dose on the COD removal.

3.4. Effect of the pH at different contact time

The effects of the pH were conducted as one of the factors that could affect the degradation of CPF wastewater. The pH was ranging from 4.5 to 10 and Ag/AgBr/TiO_2 was kept fixed at 1 g. From Fig. 3a COD removal was significant in the acidic medium and declined when the pH shifted to an alkaline medium. This indicates that the COD removal was favored in acidic condition. This agrees with work by Amalraj and Pius

Table 4
Sequential model fitting for CPF wastewater treatment

Source	Sum of squares	Degree of freedom	Mean square	F-value	P-value	Remark
Sequential model sum of squares						
Mean	1.838e + 5	1	1.838e + 5			
Linear	64.98	3	21.66	4.75	0.0097	
2FI	59.29	3	19.76	8.28	0.0008	Suggested
Quadratic	10.20	3	3.40	1.53	0.2401	
Cubic	17.43	4	4.36	2.71	0.0730	Aliased
Residual	22.49	14	1.61			
Total	1.840e + 5	28	6571.28			
Lack of fit tests						
Linear	89.41	11	8.13	5.28	0.0030	
2FI	30.12	8	3.77	2.45	0.0732	Suggested
Quadratic	19.92	5	3.98	2.59	0.0775	
Cubic	2.49	1	2.49	1.62	0.2259	Aliased
Pure error	20.00	13	1.54			
Source	Standard deviation	R ²	Adj R ²	Predicted R ²	PRESS	Remarks
Model summary statistics						
Linear	2.14	0.3726	0.2942	0.1150	154.33	
2FI	1.54	0.7126	0.6305	0.4469	96.47	Suggested
Quadratic	1.49	0.7711	0.6566	0.2642	128.33	
Cubic	1.27	0.8711	0.7513	-0.3287	231.72	

Table 5
ANOVA for response surface 2FI model

Source	Sum of squares	Degree of freedom	Mean squares	F-value	P-value	Remark
Model	124.27	6	20.71	8.68	<0.0001	Significant
Residual	50.12	21	2.39			
Lack of fit	30.12	8	3.77	2.45	0.0732	Not significant
Pure error	20.00	13	1.54			
Corr. total	174.39	27				

Table 6
Coefficient of the regression model and their significance

Factor	Coefficient estimate	Degree of freedom	Standard error	F-value	95% confidence interval low	95% confidence interval high	P-value
Intercept	81.03	1	0.29	–	80.42	81.63	–
A-pH	-1.51	1	0.32	23.00	-2.17	-0.86	<0.0001
B-time	0.65	1	0.32	4.19	-9.976e-3	1.30	0.0533
C-catalyst dosage	-0.054	1	0.32	0.030	-0.71	0.60	0.8653
AB	1.27	1	0.39	10.79	0.47	2.07	0.0035
AC	0.34	1	0.39	0.79	-0.46	1.15	0.3835
BC	-1.41	1	0.39	13.26	-2.21	-0.60	0.0015

[40]. In alkaline medium, COD removal increased with time. This was due to the generation of hydroxyl radical [41] in the alkaline medium and attracted the contaminant with positive charge [42–44]. This indicates that the effectiveness of the COD removal can be achieved by elongating the reaction time.

3.5. Effect of Ag/AgBr/TiO₂ dose

The effects of the photocatalyst dose on the degradation of CPF wastewater were studied ranging from 0 to 2.5 g in 100 ml of the CPF wastewater. From Fig. 3b, COD removal increased with increasing photocatalyst dosage and contact

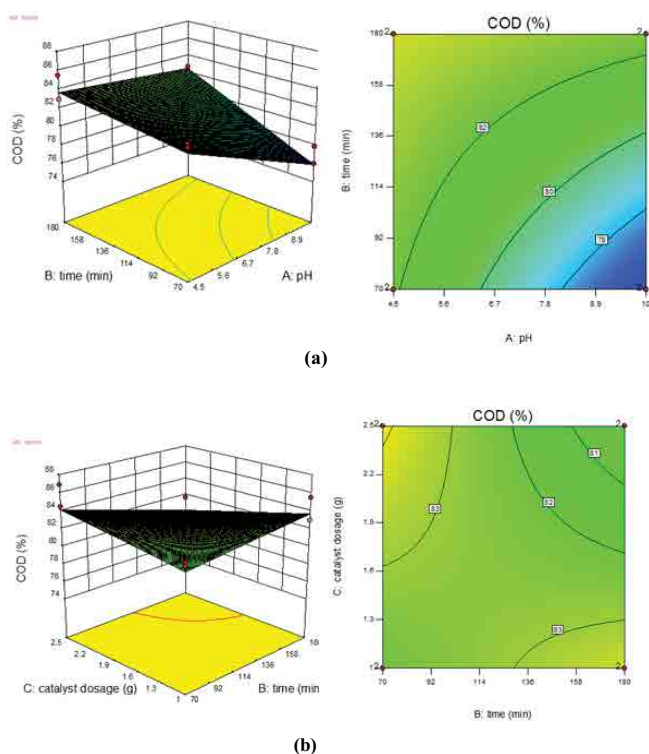


Fig. 3. Effects of catalyst dosage, pH and time on the percentage of COD removal. (a) Catalyst dosage was kept constant at 1 g and (b) pH was kept constant at 4.5.

time. This was because the increasing photocatalyst provided a larger surface area of contact with CPF wastewater. Meanwhile, the formation of the electron-hole pairs and reactive hydroxyl radical particles increased when Ag/AgBr was doped on the surface of TiO_2 . However, COD removal slightly dropped (80%) when 3.25 g of the photocatalyst was used in the reaction. This may be due to the agglomeration of the photocatalyst which hindered the active side of the photocatalyst. Otherwise, an excess amount of photocatalyst increased the turbidity of the CPF wastewater and thus inhibited the light to reach the CPF solution [34].

3.6. Optimization and validation of CPF wastewater photodegradation

In order to optimize the operating conditions of CPF wastewater degradation, the design expert selected the most desirable conditions for COD removal. The model predicted that 82.1% of COD would be removed with about 1.0 g of Ag/AgBr/ TiO_2 , at pH 4.5 and 70 min stirring time. In order to confirm the predicted COD removal efficiency, experiments were conducted in duplicates under the optimum condition and the results revealed that the average COD removal was 78.5%, corresponding well to the predicted result (Table 7).

3.7. High-performance liquid chromatography

Based on the HPLC study, the concentration of CPF active ingredient in the wastewater was degraded up to 52.9% under optimized conditions. It was noticed that the peak

Table 7
Predicted and experimental values of the responses at optimum conditions

pH (min)	Optimum conditions		COD removal (%)	
	Contact time (min)	Ag dosage (g)	Experimental	Predicted
4.5	70	1	79	82.1
4.5	70	1	78	82.1
Average:			78.5	82.1

(3.931) for the standard grade of CPF was similar to the peak (3.918) of commercial CPF (concentration = 38.7 w/w%). It was observed that the height of the peak of commercial CPF and another unknown peak (2.415) reduced after the photocatalytic test showing that the Ag/AgBr/ TiO_2 performed well as a photocatalyst which was activated using visible light (Fig. 4). The area of the commercial CPF 1990.05 was reduced to 936.25 and the concentration of commercial CPF was degraded to 52.9% indicating that CPF was degraded.

3.8. Kinetic study

The pseudo-first-order kinetic was obtained by plotting the graph of $\ln(C_0/C)$ vs. time as shown in Fig. 5. The reaction rate constant (k) determined from the slope of the graph [45] was 0.0051 min^{-1} while the R^2 was 0.6454.

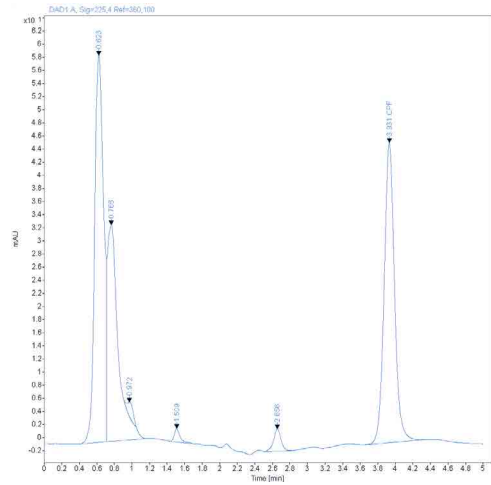
The low R^2 value obtained from the pseudo-second-order as shown in Fig. 6 indicated that pseudo-second-order reaction was not well suited to describe the rate of degradation of CPF wastewater by Ag/AgBr/ TiO_2 . Pseudo-second-order reaction did not occur as there were no two active sites for a catalyst to absorb one adsorbate molecule [46]. The summary of the kinetic parameter and coefficient of determination (R^2) from the pseudo-first-order and pseudo-second-order models are shown in Table 8. The rate of degradation of CPF with Ag/AgBr/ TiO_2 fit better to the pseudo-first-order reaction in comparison to the pseudo-second-order reaction.

3.9. Stability and reusability of Ag/AgBr/ TiO_2 catalyst

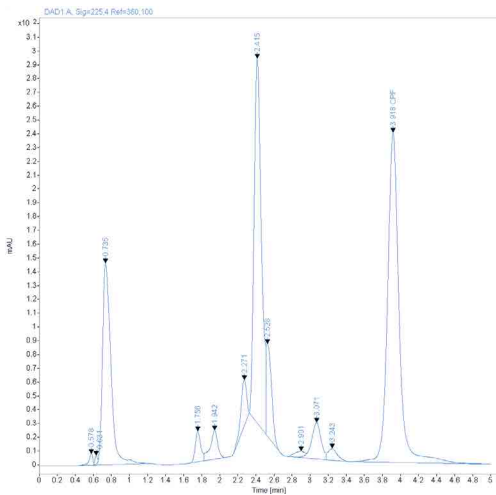
The stability and reusability of the photocatalyst are important as they can reduce the operation cost. To study the stability of Ag/AgBr, the experimental processes were carried out three times. Ag/AgBr/ TiO_2 was settled, filtered with distilled water and dried in the oven before each treatment. Fig. 7 shows that the Ag/AgBr/ TiO_2 was stable during the photocatalytic process as the spectra were nearly identical. The first, second and third efficiency were 78.5%, 75.5%, and 72.8%, respectively when reused for treatment.

3.10. Mechanism of the photocatalytic process

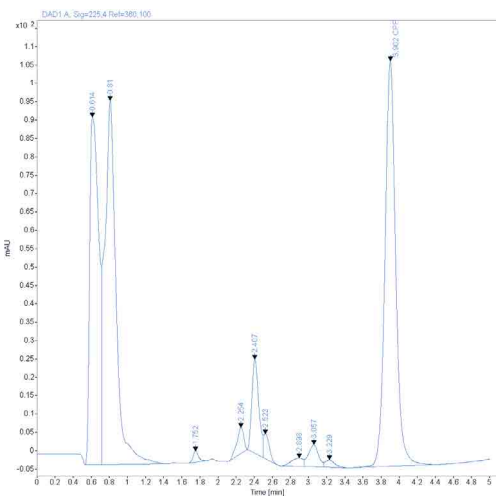
Ag and AgBr were the photoactive species, photoexcited under visible light produced electrons and holes. The dipolar characteristic of the SPR of Ag made it decay into charge carriers, electrons, and holes by photoinduction plasmons on the surface of Ag. The generated electron of Ag possibly flowed to the conduction band (CB) of TiO_2 as the position of its CB was lower than TiO_2 [22,23]. The oxygen gas on the surface



(a)



(b)



(c)

Fig. 4. HPLC diagram of (a) standard, (b) commercial, and (c) treated CPF with Ag/AgBr/TiO₂.

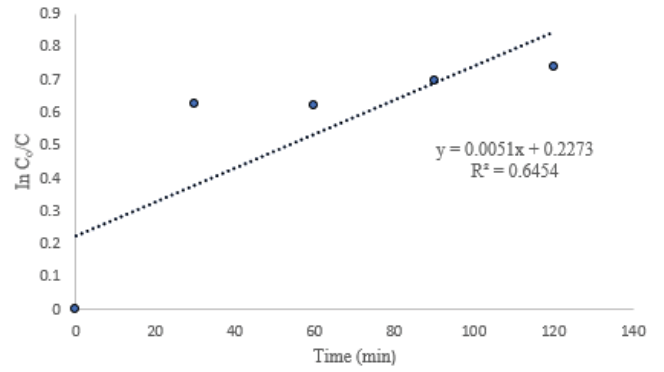


Fig. 5. Kinetics of COD removal by the pseudo-first-order reaction.

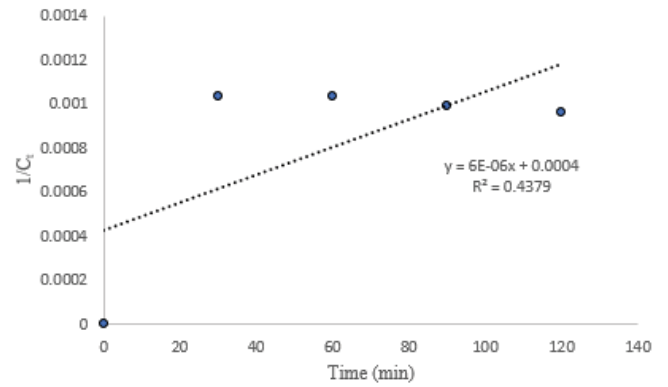


Fig. 6. Kinetics of COD removal by the pseudo-second-order reaction.

Table 8
Pseudo-first-order and pseudo-second-order model constants for the COD removal

Pseudo-first-order		Pseudo-second-order	
k (L min ⁻¹)	R^2	k (L min ⁻¹)	R^2
0.0051	0.6454	0.000006	0.4379

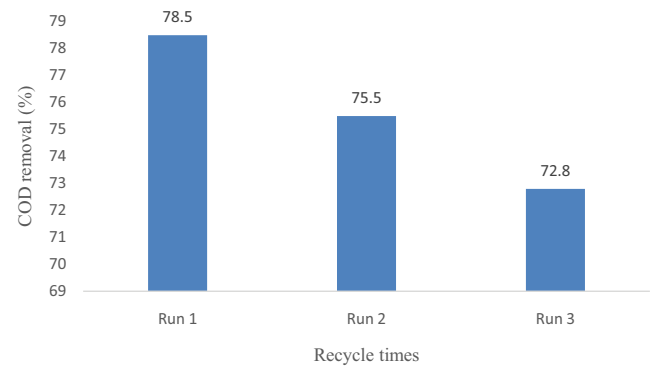
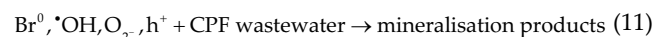
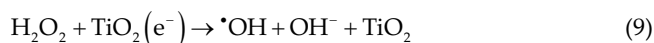
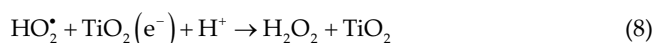
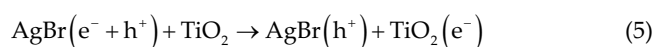
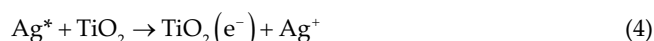


Fig. 7. Reusability of Ag/AgBr/TiO₂ for degradation of CPF wastewater.

of the TiO_2 reacted with the electrons to form O_2^- and further formed $\cdot\text{OH}$ [39,47]. Simultaneously, plasmon-induced holes from Ag and AgBr trapped on the surface of AgBr particles consequently led to the charge separation in Ag particles. The photoinduced holes on the surface of AgBr furthered oxidized the Br^- to Br^0 , another reactive radical which oxidized CPF directly and it reduced to Br^- after the reaction [22,23]. Eqs. (2)–(11) shows the relevant reactions occurring at the surface of Ag-AgBr/ TiO_2 .



4. Conclusion

The Ag/AgBr/ TiO_2 at a ratio of 1:1 (Ag: TiO_2) produced by impregnation–precipitation–photoreduction was used to treat the CPF pesticide wastewater. Statistical optimization was done using RSM with CCD tool and the results indicated that the 2FI model was significant for Ag/AgBr/ TiO_2 in the treatment of CPF wastewater. Parameters such as pH, contact time and catalyst dose were studied and the model showed that only pH input factor affected the removal efficiency as its *P*-value was less than 0.0001. However, the interaction of pH and contact time and interaction of pH and catalyst dose showed significant effects in the degradation of the CPF pesticide. The prepared photocatalyst could be used as much as three times lowering material separation cost. This study showed that titanium dioxide activation by UV light could be replaced by visible light to help reduce operating costs.

Acknowledgment

This work was supported by the University College of Technology Sarawak (UCTS) [UCTS/RESEARCH/3/2018/09].

References

- [1] R. Serrano, F.J. López, A. Roig-Navarro, F. Hernández, Automated sample clean-up and fractionation of chlorpyrifos, chlorpyrifos-methyl and metabolites in mussels using normal-phase liquid chromatography, *J. Chromatogr. A*, 778 (1997) 151–160.
- [2] M. Ismail, H.M. Khan, M. Sayed, W.J. Cooper, Advanced oxidation for the treatment of chlorpyrifos in aqueous solution, *Chemosphere*, 93 (2013) 645–651.
- [3] D.M. Whitacre, *Reviews of Environmental Contamination and Toxicology*, Vol. 202, Springer, Spain, 2009.
- [4] M.A. Randhawa, F.M. Anjum, A. Ahmed, M.S. Randhawa, Field incurred chlorpyrifos and 3,5,6-trichloro-2-pyridinol residues in fresh and processed vegetables, *Food Chem.*, 103 (2007) 1016–1023.
- [5] S. Malato, J. Blanco, J. Cáceres, A.R. Fernández-Alba, A. Agüera, A. Rodríguez, Photocatalytic treatment of water-soluble pesticides by photo-Fenton and TiO_2 using solar energy, *Catal. Today*, 76 (2002) 209–220.
- [6] M. Yadav, N. Srivastava, R.S. Singh, S.N. Upadhyay, S.K. Dubey, Biodegradation of chlorpyrifos by *Pseudomonas* sp. in a continuous packed bed bioreactor, *Bioresour. Technol.*, 165 (2014) 265–269.
- [7] R. Saini, P. Kumar, Simultaneous removal of methyl parathion and chlorpyrifos pesticides from model wastewater using coagulation/flocculation: central composite design, *J. Environ. Chem. Eng.*, 4 (2016) 673–680.
- [8] S. Malato, P. Fernández-Ibáñez, M.I. Maldonado, J. Blanco, W. Gernjak, Decontamination and disinfection of water by solar photocatalysis: recent overview and trends, *Catal. Today*, 147 (2009) 1–59.
- [9] J.G. McEvoy, Z.S. Zhang, Synthesis and characterization of Ag/AgBr-activated carbon composites for visible light induced photocatalytic detoxification and disinfection, *J. Photochem. Photobiol., A*, 321 (2016) 161–170.
- [10] A.L.N. Mota, L.F. Albuquerque, L.T.C. Beltrame, O. Chivone-Filho, A. Machulek Jr., C.A.O. Nascimento, Advanced oxidation processes and their application in the petroleum industry: a review, *Braz. J. Pet. Gas*, 2 (2008) 122–142.
- [11] C.-Y. Wang, X. Zhang, X.-N. Song, W.-K. Wang, H.-Q. Yu, Novel $\text{Bi}_{12}\text{O}_{15}\text{Cl}_6$ photocatalyst for the degradation of bisphenol A under visible-light irradiation, *ACS Appl. Mater. Interfaces*, 8 (2016) 5320–5326.
- [12] B. Paul, A. Locke, W.N. Martens, R.L. Frost, Decoration of titania nanofibres with anatase nanoparticles as efficient photocatalysts for decomposing pesticides and phenols, *J. Colloid Interface Sci.*, 386 (2012) 66–72.
- [13] Y.J. Li, L.M. Yu, N. Li, W.F. Yan, X.T. Li, Heterostructures of $\text{Ag}_3\text{PO}_4/\text{TiO}_2$ mesoporous spheres with highly efficient visible light photocatalytic activity, *J. Colloid Interface Sci.*, 450 (2015) 246–253.
- [14] X.Y. Li, D.S. Wang, G.X. Cheng, Q.Z. Luo, J. An, Y.H. Wang, Preparation of polyaniline-modified TiO_2 nanoparticles and their photocatalytic activity under visible light illumination, *Appl. Catal., B*, 81 (2008) 267–273.
- [15] R. Asahi, T. Morikawa, T. Ohwaki, K. Aoki, Y. Taga, Visible-light photocatalysis in nitrogen-doped titanium oxides, *Science*, 293 (2001) 269–271.
- [16] C.K. Cheng, M.R. Derahman, M.R. Khan, Evaluation of the photocatalytic degradation of pre-treated palm oil mill effluent (POME) over Pt-loaded titania, *J. Environ. Chem. Eng.*, 3 (2015) 261–270.
- [17] P. Wang, B.B. Huang, X.Y. Qin, X.Y. Zhang, Y. Dai, J.Y. Wei, M.-H. Whangbo, Ag@AgCl: a highly efficient and stable photocatalyst active under visible light, *Angew. Chem. Int. Ed.*, 47 (2008) 7931–7933.
- [18] K. Fuku, R. Hayashi, S. Takakura, T. Kamegawa, K. Mori, H. Yamashita, The synthesis of size- and color-controlled silver nanoparticles by using microwave heating and their enhanced catalytic activity by localized surface plasmon resonance, *Angew. Chem.*, 125 (2013) 7594–7598.
- [19] P. Wang, B.B. Huang, Q.Q. Zhang, X.Y. Zhang, X.Y. Qin, Y. Dai, J. Zhan, J.X. Yu, H.X. Liu, Z.Z. Lou, Highly efficient visible light plasmonic photocatalyst Ag@Ag(Br,I), *Chem. Eur. J.*, 16 (2010) 10042–10047.
- [20] M.R. Elahifard, S. Rahimnejad, S. Haghghi, M.R. Gholami, Apatite-coated Ag/AgBr/ TiO_2 visible-light photocatalyst for destruction of bacteria, *J. Am. Chem. Soc.*, 129 (2007) 9552–9553.

- [21] C. Hu, T. Peng, X. Hu, Y. Nie, X. Zhou, J. Qu, H. He, Plasmon-induced photodegradation of toxic pollutants with Ag-AgI/Al₂O₃ under visible-light irradiation, *J. Am. Chem. Soc.*, 132 (2010) 857–862.
- [22] Y.J. Sui, C.Y. Su, X.D. Yang, J.L. Hu, X.J. Lin, Ag-AgBr nanoparticles loaded on TiO₂ nanofibers as an efficient heterostructured photocatalyst driven by visible light, *J. Mol. Catal. A: Chem.*, 410 (2015) 226–234.
- [23] D.S. Wang, Y.D. Duan, Q.Z. Luo, X.Y. Li, J. An, L.L. Bao, L. Shi, Novel preparation method for a new visible light photocatalyst: mesoporous TiO₂ supported Ag/AgBr, *J. Mater. Chem.*, 22 (2012) 4847.
- [24] X.X. Liu, D. Zhang, B. Guo, Y. Qu, G. Tian, H.J. Yue, S.H. Feng, Recyclable and visible light sensitive Ag-AgBr/TiO₂: surface adsorption and photodegradation of MO, *Appl. Surf. Sci.*, 353 (2015) 913–923.
- [25] Y. Hou, X.Y. Li, Q.D. Zhao, G.H. Chen, C.L. Raston, Role of hydroxyl radicals and mechanism of *Escherichia coli* inactivation on Ag/AgBr/TiO₂ nanotube array electrode under visible light irradiation, *Environ. Sci. Technol.*, 46 (2012) 4042–4050.
- [26] S. Karimifard, M.R.A. Moghaddam, Application of response surface methodology in physicochemical removal of dyes from wastewater: a critical review, *Sci. Total Environ.*, 640–641 (2018) 772–797.
- [27] M. Behbahani, M.R.A. Moghaddam, M. Arami, Techno-economical evaluation of fluoride removal by electrocoagulation process: optimization through response surface methodology, *Desalination*, 271 (2011) 209–218.
- [28] M. Khedmati, A. Khodaii, H.F. Haghshenas, A study on moisture susceptibility of stone matrix warm mix asphalt, *Constr. Build. Mater.*, 144 (2017) 42–49.
- [29] H.F. Haghshenas, A. Khodaii, M. Khedmati, S. Tapkin, A mathematical model for predicting stripping potential of Hot Mix Asphalt, *Constr. Build. Mater.*, 75 (2015) 488–495.
- [30] N. Mansouriieh, M.R. Sohrabi, M. Khosravi, Optimization of profenofos organophosphorus pesticide degradation by zero-valent bimetallic nanoparticles using response surface methodology, *Arabian J. Chem.*, (2015), (In Press) <https://doi.org/10.1016/j.arabjc.2015.04.009>.
- [31] S. Mosleh, M.R. Rahimi, Intensification of abamectin pesticide degradation using the combination of ultrasonic cavitation and visible-light driven photocatalytic process: synergistic effect and optimization study, *Ultrason. Sonochem.*, 35(Pt A) (2017) 449–457.
- [32] E.E. Mitsika, C. Christophoridis, K. Fytianos, Fenton and Fenton-like oxidation of pesticide acetamiprid in water samples: kinetic study of the degradation and optimization using response surface methodology, *Chemosphere*, 93 (2013) 1818–1825.
- [33] M.H. Dehghani, Z.S. Niasar, M.R. Mehrnia, M. Shayeghi, M.A. Al-Ghouti, B. Heibati, G. McKay, K. Yetilmezsoy, Optimizing the removal of organophosphorus pesticide malathion from water using multi-walled carbon nanotubes, *Chem. Eng. J.*, 310 (2016) 22–32.
- [34] M.G. Alalm, A. Tawfik, S. Ookawara, Comparison of solar TiO₂ photocatalysis and solar photo-Fenton for treatment of pesticides industry wastewater: operational conditions, kinetics, and costs, *J. Water Process Eng.*, 8 (2015) 55–63.
- [35] WEF, APHA, Standard Methods for the Examination of Water and Wastewater, American Public Health Association (APHA), Washington, D.C., USA, 2005.
- [36] L. Shi, L. Liang, J. Ma, Y. Meng, S. Zhong, F.X. Wang, J.M. Sun, Highly efficient visible light-driven Ag/AgBr/ZnO composite photocatalyst for degrading Rhodamine B, *Ceram. Int.*, 40 (2014) 3495–3502.
- [37] Y.X. Yang, W. Guo, Y.N. Guo, Y.H. Zhao, X. Yuan, Y.H. Guo, Fabrication of Z-scheme plasmonic photocatalyst Ag@AgBr/g-C₃N₄ with enhanced visible-light photocatalytic activity, *J. Hazard. Mater.*, 271 (2014) 150–159.
- [38] X.X. Liu, D. Zhang, B. Guo, Y. Qu, G. Tian, H.J. Yue, S.H. Feng, Recyclable and visible light sensitive Ag-AgBr/TiO₂: surface adsorption and photodegradation of MO, *Appl. Surf. Sci.*, 353 (2015) 913–923.
- [39] Y. Hou, X.Y. Li, Q.D. Zhao, X. Quan, G.H. Chen, TiO₂ nanotube/Ag-AgBr three-component nanojunction for efficient photoconversion, *J. Mater. Chem.*, 21 (2011) 18067–18076.
- [40] A. Amalraj, A. Pius, Photocatalytic degradation of monocrotophos and chlorpyrifos in aqueous solution using TiO₂ under UV radiation, *J. Water Process Eng.*, 7 (2015) 94–101.
- [41] Y.-J. Chiang, C.-C. Lin, Photocatalytic decolorization of methylene blue in aqueous solutions using coupled ZnO/SnO₂ photocatalysts, *Powder Technol.*, 246 (2013) 137–143.
- [42] H.R. Rajabi, O. Khani, M. Shamsipur, V. Vatanpour, High-performance pure and Fe³⁺-ion doped ZnS quantum dots as green nanophotocatalysts for the removal of malachite green under UV-light irradiation, *J. Hazard. Mater.*, 250–251 (2013) 370–378.
- [43] F.D. Mai, C.S. Lu, C.W. Wu, C.H. Huang, J.Y. Chen, C.C. Chen, Mechanisms of photocatalytic degradation of Victoria Blue R using nano-TiO₂, *Sep. Purif. Technol.*, 62 (2008) 423–436.
- [44] N. Sobana, K. Selvam, M. Swaminathan, Optimization of photocatalytic degradation conditions of Direct Red 23 using nano-Ag doped TiO₂, *Sep. Purif. Technol.*, 62 (2008) 648–653.
- [45] H. Zhao, S.H. Xu, J.B. Zhong, X.H. Bao, Kinetic study on the photo-catalytic degradation of pyridine in TiO₂ suspension systems, *Catal. Today*, 93–95 (2004) 857–861.
- [46] M.V. Subbaiah, D.-S. Kim, Adsorption of methyl orange from aqueous solution by aminated pumpkin seed powder: kinetics, isotherms, and thermodynamic studies, *Ecotoxicol. Environ. Saf.*, 128 (2016) 109–117.
- [47] X. Chen, Z.F. Zheng, X.B. Ke, E. Jaatinen, T.F. Xie, D.J. Wang, C. Guo, J.C. Zhao, H.Y. Zhu, Supported silver nanoparticles as photocatalysts under ultraviolet and visible light irradiation, *Green Chem.*, 12 (2010) 414–419.